Design and Joint Control of a Conjoined Biplane and Quadrotor

Schröter, S.; Smeur, E.J.J.; Remes, B.D.W.

DOI
10.1142/S2301385024430039

Publication date
2023

Document Version
Accepted author manuscript

Published in
Unmanned Systems

Citation (APA)
Schröter, S., Smeur, E. J. J., & Remes, B. D. W. (2023). Design and Joint Control of a Conjoined Biplane and Quadrotor. *Unmanned Systems*, *12*(3), 579-588. https://doi.org/10.1142/S2301385024430039

Unmanned Systems, Vol. 0, No. 0 (2013) 1–9

Design and Joint Control of a Conjoined Biplane and Quadrotor

S.Schröter, E.J.J.Smeur, B.D.W. Remes

University Department, Delft University of Technology, Kluyverweg 1, 2629 HS, the Netherlands
E-mail: shawn@schroter.info

Unmanned Aerial Vehicles (UAVs) have the potential to perform many different missions, some of which may require a large aircraft for endurance and a small aircraft for maneuverability in wind gusts or cluttered environments, such as buildings. This paper proposes a novel combination of a quadrotor and a hybrid biplane capable of joint hover, joint forward flight, and mid-air separation followed by separate flight. We investigate cooperative control strategies during joint flight that do not require any communication between the quadcopter and the biplane. This means that the two aircraft have their own independent control strategy based on their own sensors. The biplane, which is the largest of the two with most control authority, leads the flight and the goal for the quadrotor is to help in producing thrust and increasing rotational stability. Three control strategies for the quadrotor are compared: a proportional angular rate damper, a proportional angular acceleration damper, and constant thrust without attitude control. Simulation and practical tests show that for desired attitude changes of the biplane, the quadrotor rate- and angular acceleration damper strategies lead to a small performance degradation. However, the angular rate damper strategy reduces the roll angle error in disturbance rejection experiments and requires the smallest input command. The in-flight release is successfully tested in joint hover up to a forward pitch angle of -18 [deg].

Keywords: in-flight release; joint flight; tailsitter; quadrotor; hybrid biplane; INDI.

1. Introduction

Unmanned Air Vehicles (UAVs) have increased in popularity and can serve various purposes, ranging from inspection of structures to traffic surveillance, and each type of UAV has its own distinguishing properties. Fixed-wing aircraft are known for their endurance and efficiency, but they require a constant horizontal speed to stay in the air. Multirotors are more agile and are capable of hover, but they lack endurance. A hybrid aircraft can hover and has wings for efficient forward flight, combining the best of both worlds. However, a hybrid aircraft with large wings is not well-equipped to maneuver inside a building. This poses a problem for missions where the goal is to fly inside a building after a long-distance transit flight.

One solution could be to drop a smaller UAV out of a bigger one. In-air deployment of a fixed-wing from a quadrotor has been shown by Boeing[a]. Voskuijl et al. investigated morphing UAVs being dropped as armaments out of (military) airplanes.[1] A downside of this approach is that the smaller UAV is carried around as dead weight, and does not contribute to the propulsion until it is deployed. This could lead to over-dimensioning of the carrier aircraft. Cooperative flight is somewhat similar to airborne docking,[2] formation flight with communication,[3] and without communication.[4] However, in these works the individual UAVs are typically not rigidly attached and can maneuver independently to some degree.

Examples of cooperative flight with modular joint airframes are the Modquad[5] and the Distributed Flight Array.[6] Both airframes are capable of assembling in-flight, and the latest version of the Modquad is even capable of in-flight disassembly.[7] However, all aircraft used in this research have the same size and function, without a focus on combining different types of UAVs to obtain better endurance and flexibility in operation.

In this paper, we propose a combination of a quadrotor and a hybrid aircraft with a fixed wing, that can fly together, both contributing to stabilization and propulsion, and can disassemble in-flight into a fully functional quadcopter and hybrid aircraft. Figure 1 graphically shows the various stages in which the joint structure would fly.

For a UAV's attitude and trajectory control specifically, many options exist. The most popular method is Proportional Integral Derivative (PID) control,[8] but also model-based controllers exist for UAVs.[9] For hybrid air-

[a] `https://www.boeing.com/features/2016/09/catch-and-release-flares-09-16.page`

craft, Incremental Nonlinear Dynamic Inversion (INDI) has proven to be very effective.[10] Especially in the hover phase, hybrid aircraft are extremely susceptible to external disturbances,[11,12] and INDI has better disturbance rejection compared to PID.[13]

In the formation flight literature discussed above, the communication between drones has proven to pose challenges, such as time delays, false information, and noise. Wired communication between the aircraft would be less of a liability, but a way to work around all these problems is to avoid any communication altogether. That is why a control strategy is proposed in this paper where both aircraft have no communication with each other. This way, the joint structure becomes more reliable, which is important for long-distance operations.

The contribution of this paper is twofold: (1) a proposed method of in-air separation of two rigidly-attached heterogeneous UAVs, and (2) a comparison of performance and stability of the vehicle, considering different control strategies for the quadrotor without communication with the biplane.

(a) Joint Hover. (b) Joint Forward flight.

(c) In-flight release. (d) The quadrotor maneuvering in a building, while the biplane loiters as a data relay station.

Fig. 1. Rendering of different phases of a typical flight.

2. Joint structure design

This section will cover three main parts of the structure in more detail: The hybrid biplane, the quadrotor and the release mechanism.

2.1. *Hybrid biplane*

The biplane is a tailsitter hybrid aircraft, for which the Nederdrone[10] formed the basis of the design. The biplane has eight mounting points for rotors and four control surfaces. The four outer mounting points are fixed, and the four inner mounting points are part of the release mechanism. The control surfaces manipulate the airflow around the wings, providing moments around the body Y- and Z-axes. In the hover phase, this airflow is created by the rotors. Table 1 presents an overview of the different parts of the hybrid biplane. The body reference frame is defined in hover state, as shown in Figure 2(a). Adopting the ZXY Euler angle rotation order, forward flight is achieved through a -90 deg pitch angle.

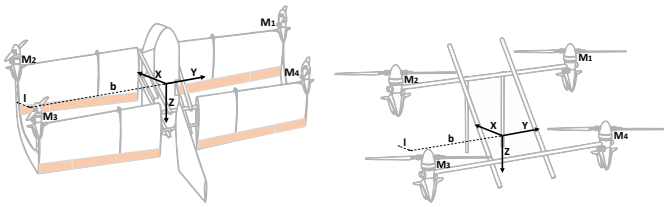

(a) Hybrid biplane (b) Quadrotor

Fig. 2. Drawings of the hybrid biplane and quadrotor with body axis definitions. The control surfaces are accentuated in light orange.

Table 1. Different components of the biplane

Type of Hardware	**Brand**	**Item**
Motor	T-Motor	MN3510
Radio Control link	TBS	Crossfire nano
Telemetry link	Herelink	Herelink
Electronic Speed Controller	T-Motor	f45A 32_bit
Propeller	T-motor	MF1302
Flight controller	Holybro	Pixhawk4
Battery	Extron	2x 6s 4.5 Ah

2.2. *Quadrotor*

The design of the quadrotor is derived from the dimensions of the biplane, such that the four motors of the quadrotor fit exactly on the four mounting points of the biplane. Four hollow carbon rods connect the four rotors. The rods are placed in such a way that the quadrotor would be able to release without being obstructed by the biplane. Furthermore, two solid carbon rods provide a more consistent release and serve as landing legs. A schematic overview of the quadrotor is shown in Figure 2(b). The quadrotor uses the same hardware as the biplane, described in Table 1, with the exception of the batteries, which are two 3s 4500 mAh batteries, connected in series.

To make the system more efficient, it is possible to equip the quadrotor with low-pitch folding propellers, that are efficient in hovering flight. Since during forward flight less thrust is required, these propellers can fold such that they produce little drag. The biplane can be equipped with large pitch fixed propellers, which are efficient in forward

flight when the propellers receive more inflow. These efficiency optimizations were beyond the scope of this paper.

2.3. *Release mechanism*

The release mechanism is mounted just underneath the motors of the quadrotor. At each of the four motor locations, two copper pins fix the quadrotor to the biplane. The release system is a slider-crank mechanism powered by a servo. Since the quadrotor needs to drastically change its method of control once it detaches from the biplane, it is crucial that the flight control system on the quadrotor knows when it detaches. To establish this, the quadrotor is driving the servos that control the release.

Figure 3 graphically shows how the release system enables the quadrotor to separate from the biplane. Once the pins are out, the motor mount slides in the direction of the thrust force. A thrust difference between the biplane and the quadrotor then leads to separation. The guiding tubes of the quadrotor help the thrust force of the quadrotor to stay approximately opposite to the weight force of the biplane.

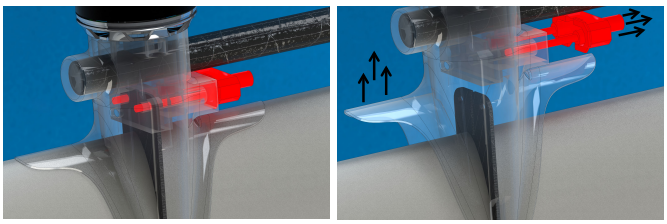

(a) Closed position - The pin is locked in the carbon plate. (b) Lift-off of the quadrotor.

Fig. 3. Closed position and release of the RC servo Release Mechanism

3. Flight control

Both aircraft will be flying in three different flight phases: joint hover, joint forward flight, and separate hover. This paper focuses on a control law for both hover phases, since joint forward flight can only be achieved after the joint hover phase is properly controlled.

3.1. *Incremental Nonlinear Dynamic Inversion*

For the flight control strategy, INDI is chosen as a starting point. It has been proven that INDI can perform well for tailsitter hybrid aircraft. These aircraft have complex aerodynamics during the different flight phases and are very sensitive to wind gusts in hover. INDI treats modeling errors as disturbances, to which it has good rejection capabilities.[10,13] The following gives a brief overview of the control method, but the interested reader is referred to the work by Smeur et al.[13] For both aircraft the following angular momentum equation holds:

$$\begin{aligned} M &= I_v\dot{\Omega} + \Omega \times I_v\Omega \\ &= M_a(\Omega, v) + M_c(\omega) + M_r(\omega, \dot{\omega}, \Omega), \end{aligned} \tag{1}$$

where M is the total moment, I_v is the inertia matrix of the vehicle, ω is the angular rate of the propellers around the body Z-axis and $\dot{\omega}$ is the angular acceleration of the propellers around the body Z-axis. M_a is the aerodynamic moment on the vehicle, M_c is the moment due to motor commands, M_r is the moment due to the gyroscopic effect of the rotors and Ω is the angular velocity vector.

Following the procedure of Smeur et al.,[14] we linearize Eq. (1) using a Taylor expansion, and the gyroscopic effects of the rotors are neglected and changes in aerodynamic moments are assumed to be small with respect to changes in control moments:

$$\dot{\Omega} = \dot{\Omega}_0 + G_1(\omega - \omega_0) + T_s G_2(\dot{\omega} - \dot{\omega}_0), \tag{2}$$

where T_s is the sample time of the discrete time controller, G_1 is the linearized control effectiveness of the actuators, G_2 is the linearized propeller inertia effect on the angular acceleration in the Z-axis.

In order to remove the dependency on both ω and $\dot{\omega}$, we apply the discrete time approximation $\dot{\omega} = (\omega - \omega z^{-1}){T_s}^{-1}$. We also consider that the signal $\dot{\Omega}_0$ is in fact the angular acceleration at the previous timestep, which has to be obtained from taking a finite difference of the gyroscope signal. As this signal is typically very noisy, it has to be filtered with a low pass filter, which we denote with the subscript f. This introduces a delay, and in order for the Taylor expansion to be correct, all terms with subscript 0 need to be filtered with the same filter.

Inverting Eq. 2 for ω we arrive at an INDI control law:

$$\omega_c = \omega_f + (G_1 + G_2)^{+}(v - \dot{\Omega}_f + G_2 z^{-1}(\omega_c - \omega_f)), \tag{3}$$

where we have given the new actuator command with the subscript c, and v is the virtual control input, which is the reference angular acceleration generated by a PD controller.

3.2. *Control authority analysis*

To analyze how the two aircraft compare considering control authority, the control moment from Eq. (1) is used. The control moment, M_c, is defined for a quadrotor as:[15]

$$M_c = \begin{bmatrix} -bk_1 & bk_1 & bk_1 & -bk_1 \\ lk_1 & lk_1 & -lk_1 & -lk_1 \\ k_2 & -k_2 & k_2 & -k_2 \end{bmatrix} \omega^2, \tag{4}$$

where b is the lateral distance from the Center of Gravity (CG) to the rotors, l is the longitudinal distance between the CG and the rotors, as shown in Figure 2. k_1 is the force constant of the rotors, k_2 is the moment constant of the rotors, and ω is the angular rate vector of the rotors.

From Eq. (4) the control effectiveness of the different actuators can be derived. The actuator force constants are the same for the biplane and the quadrotor, since the same hardware is used for both aircraft. During the hover phase,

the dynamic pressure is very low, such that the moment from the control surfaces can be neglected in comparison to the moments generated by the rotors. Then, both the biplane and the quadrotor separately can be seen as two quadrotors, where Eq. (4) describes the control moments.

Table 2. Distances.

	b	l
Biplane	0.74 [m]	0.11 [m]
Quadrotor	0.32 [m]	0.11 [m]

By comparing the values of b and l in Table 2, it can be observed that around the roll axis the biplane has more control authority than the quadrotor from the propellers alone, and the effectiveness is equal in the other axes. Considering that the biplane is also equipped with aerodynamic control surfaces, which yield additional control effectiveness, the total biplane's control authority in pitch and yaw exceeds that of the quadrotor. In conclusion, in all rotational directions the biplane has more control authority than the quadrotor.

4. Control strategies for the quadrotor in joint hover

One of the main challenges of the project is to achieve the goal without intercommunication. If both UAVs track a reference attitude, this leads to the difficulty of synchronization of the reference and (different) sensor errors, potentially leading to a differing attitude estimation. An error in synchronization or sensor measurement differences could lead to the UAVs commanding opposite control inputs. In the interest of simplicity, and given that the biplane has the most control authority, only the biplane is given a reference attitude to track.

Still, there could exist a feedback law on the quadrotor that improves the overall performance of the joint structure. Firstly, tracking performance and disturbance rejection behavior is preferred for tailsitter platforms like the biplane. Secondly, the input commands should be as small as possible, to be most efficient. Less required input command also means that the actuators are further away from their saturation point, giving the actuators more room for extra maneuvering.

The simplest strategy for the quadrotor is to provide a constant thrust, without creating any control moments. This makes the biplane fully responsible for the attitude control and adjusting the total amount of thrust. This control strategy will be referred to as *constant thrust*.

Due to the lack of communication, a major challenge for the quadrotor is to distinguish between intended changes in attitude or an external disturbance changing the attitude. Intended behavior is created by changing reference signals, stemming from an outer-loop position controller or manual input from an RC controller. Unintended behavior is usually the result of external forces acting on the platform, for instance due to wind gusts. We will investigate if the quadrotor can improve the overall performance by resisting rotations, even though that means resisting intended rotations as well, through the *angular rate damper* and *angular acceleration damper* strategies. These strategies will resist angular rates and angular accelerations respectively. The type of control is proportional control, as adding an integrator could lead to a steady state of opposing moments of the quadrotor and biplane.

In order to analyze the controller using linear systems theory, the system is linearized and a block diagram of a single axis is shown for the three strategies in Figure 4. Here, η represents an attitude angle (for instance the roll angle), and $H(s)$ is a second order Butterworth low pass filter with a cutoff frequency of 3.2 Hz. With the damper strategies, both the biplane and the quadrotor will detect a disturbance and will try to steer against this, though the quadrotor will also detect the intended behavior of the biplane as a disturbance. One could imagine that from the perspective of the biplane, the different quadcopter control strategies present the biplane controller with different system dynamics to control: for instance a system with more damping in the case of the angular rate damper strategy.

4.1. *Control group for base reference*

In order to compare the effect of the different quadrotor control strategies, performance has to be tested against a base reference. This base reference is one INDI attitude controller directly controlling *all eight rotor actuators and the control surfaces*. This makes the control group physically different from the three investigated control strategies for the quadrotor. For this strategy to work, the motors of the quadrotor are directly wired to the biplane. In the next sections this base reference is referred to as the *control group*.

4.2. *Stability analysis*

Figure 5 shows a Nichols plot derived for the different control strategies. This plot is created for the entire joint structure controller, as displayed in Figure 4. The goal is to have the system's frequency response be as far from the critical point, the red cross, in the middle. The vertical distance from the system's frequency response to the critical point illustrates the gain margin, and the horizontal distance defines the phase margin. It becomes clear that the angular acceleration damper strategy is the least robust, closely followed by the constant thrust strategy. The control group overlaps again with the constant thrust strategy. The angular rate damper is the most robust, showing better gain and phase margins than the control group.

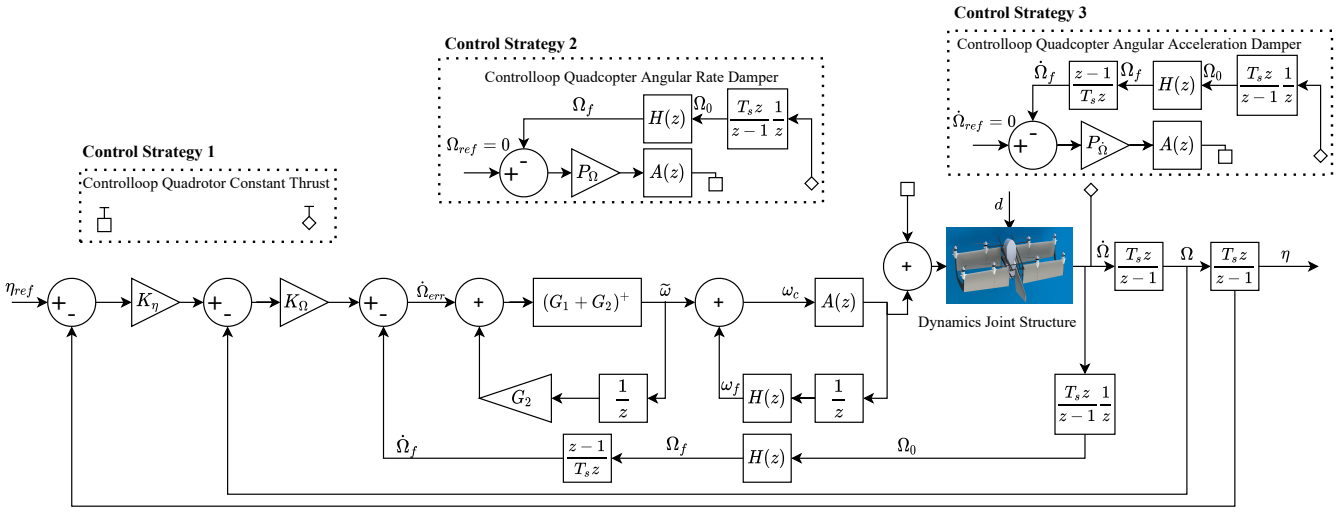

Fig. 4. Three control strategies for the quadrotor. The lower section of the loop shows the INDI cascaded attitude controller of the biplane. The area within the dotted line resembles the control loop for the quadrotor.

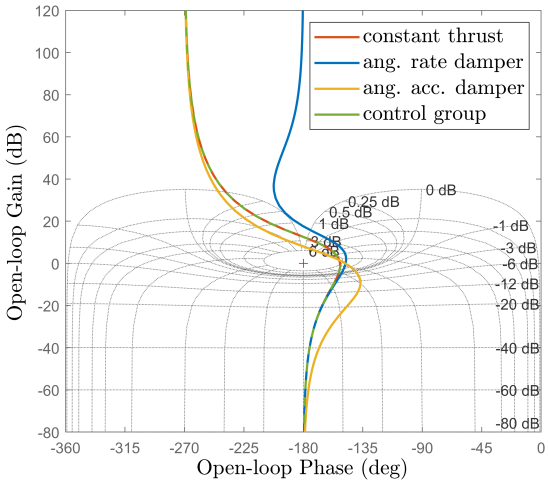

Fig. 5. Nichols plot for three strategies. Constant thrust and the control group overlap. The angular rate damper strategy should provide the best stability.

5. Practical verification

This section is focused on the joint structure's release mechanism and the test sequence for the control strategies. The test sequence has been simulated in Matlab prior to the practical flights. Videos from some of the practical tests can be seen on YouTube [b].

5.1. *Release procedure*

The design of the release mechanism was covered in Section 2. The release sequence is shown in Figure 6. It is important to note that the quadrotor does not control its attitude during the release. This is because the motor mount of the quadrotor has to slide off a carbon plate, as shown in Figure 3, and if a moment is applied this causes friction. If the quadrotor was using attitude control, or even one of the damper strategies, it could steer against the biplane and through the generated moment obstruct proper detachment.

The release procedure was tested in static tests as well as during flight tests. On average, the quadrotor was clear of the biplane in 0.39 [*sec*]. The total delay time before activation of the INDI attitude controller of the quadrotor was therefore set to 0.5 [*sec*]. This left enough time for the quadrotor to be clear of the biplane and not be in free flight for too long without active attitude control. The set-up was tested with varying forward pitch angles up to $\theta = -18$ [*deg*]. At 70% thrust, the quadrotor consistently released well.

During the flight tests, the biplane was controlled by a separate pilot using an RC controller. At the moment of release, the goal was to be as close as possible to $[\phi, \theta] = [0, 0]$ degrees. Figure 7 shows the three phases of the in-flight release. Next, both platforms were proven to be capable of separate flight. In the case of the biplane, hover flight was carried out with the four outer rotors and the control surfaces.

[b] https://www.youtube.com/playlist?list=PL_KSX9GOn2P-CC3EMxPdcHmTd-evJcLzY

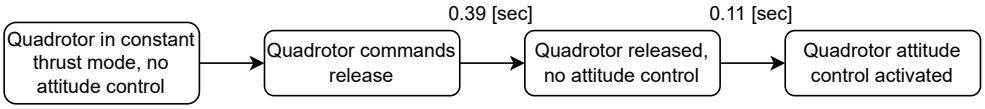

Fig. 6. Flowchart of the release mechanism

(a) Joint hover; Biplane in attitude INDI and quadrotor constant 70% thrust.

(b) Release mechanism is engaged; The quadrotor has no attitude control.

(c) Separate flight; Both aircraft are in attitude control.

Fig. 7. Field release test.

The biplane was tuned for flight with the quadrotor attached. This means that, for the calculated control effectiveness, the inertia of the joint structure is taken into account, including the mass of the quadrotor. When the quadrotor releases, the actual control effectiveness increases due to the decreased inertia. This effectively leads to an increase in gain in the closed loop system. According to Figure 5, there is some degree of robustness to such a gain change. In practice the flight performance of the biplane without the quadrotor proved adequate. One reason could be that the weight of the quadrotor is close to the CG, which only leads to a small change in inertia once the quadrotor detaches. Also, the INDI controller is naturally strong at counteracting the disturbance that could arise from a sudden shift in CG, as has been shown in previous work.[14]

5.2. *Control strategies - test setup*

Two experiments were performed: one to test the tracking performance and one to test disturbance rejection. For the first experiment, the intentional step input was initialized via the RC controller. The step was set to $\phi = 18\,[deg]$ in both positive and negative roll angles.

The experiments were performed indoors to avoid any influence of wind. In all cases, the thrust level of the quadrotor was set to 70%. Table 3 shows the mean throttle levels of the biplane for the various configurations.

In order to create a repeatable and consistent step disturbance a weight was dropped from the joint structure. Two identical weights of 672 $[g]$ each are mounted on the sides of the biplane, one weight on each side. This creates a net zero moment on the roll axis, not changing the CG, in the beginning of the test. The release of one weight shifts the CG towards the weight that is still attached, resulting in a constant roll moment. This step disturbance is comparable to the work by Smeur et al., but they added a weight to the aircraft.[16] It is assumed that any influence due to the change in inertia due to the attached weight has similar effect for all control strategies, allowing to draw conclusions from the comparison.

The flight controller software was kept the same for the different controllers to the greatest possible extent. The actuator dynamics, the filtering, and the sensor fusion all took place in a similar fashion for the quadrotor as well as the biplane.

Table 3. Experiment throttle levels.

Mean Throttle level	Biplane	Quadrotor
control group	62.13 [%]	-
constant thrust	53.90 [%]	70 [%]
ang. rate damper	53.90 [%]	70 [%]
ang. acc. damper	54.21 [%]	70 [%]
separate flight	72.33 [%]	40 [%]

5.3. *Control strategies - test results*

Figure 8 illustrates the overall result of all the roll angle step input tests. Figure 8(a) and 8(b) show the mean response

and input command respectively of 6 repetitions for the angular rate and angular acceleration damper strategies, 5 repetitions for the control group and 3 repetitions for the constant thrust strategy. Table 5 and 4 show relevant parameters of the step input and disturbance.

Figure 8(a) shows that the step input tests give a very similar response for all the strategies. Overshoot for all of the strategies does not go above 5% of the step angle. The desired roll angle could not be maintained for a long time, due to a lack of space in the hangar, which is why the steady-state is not yet achieved at the end of Figure 8.

The increase of the roll command in Figure 8(b) after $t = 2\,[sec]$ indicates that the joint structure needs to put in a constant roll offset to keep the roll angle at $\phi = 18\,[deg]$. This could be due to a head-up moment caused by the flapping movement of the rotors.[17]

Figure 9 shows the roll angle and the roll command during the disturbance rejection experiment. Here, more significant differences between the approaches can be observed. Table 4 summarizes the results from these figures. It can be observed that the control group has the lowest ϕ_{err}^{max} and the smallest required input command, as expected. Comparing this base reference strategy to the other strategies, we find that the constant thrust strategy requires 19% more peak input command to counteract the disturbance. The angular acceleration damper strategy performs even worse at 27% more required peak input command. The angular rate damper strategy performed the best, as it only required 11% more peak input command compared to the control group. The same order of performance can be stated for ϕ_{err}^{max} and the total energy required.

At this point, it should be borne in mind that the control group for this study acted as a base reference only, as it requires all actuators of both vehicles to be controlled from one flight control computer. Of the feasible options, the angular rate damper strategy proved to be the best.

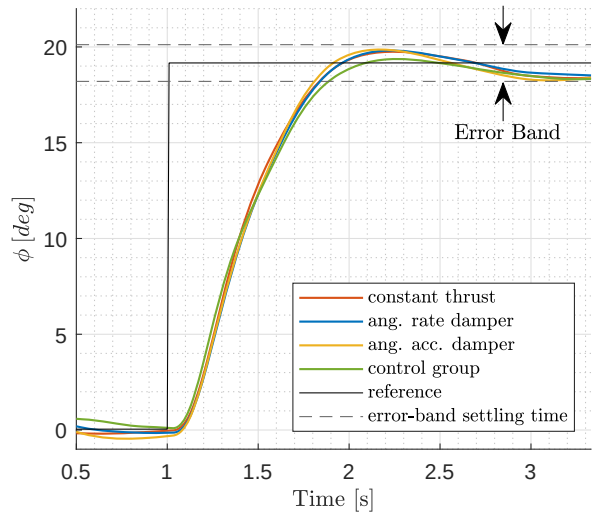

(a)

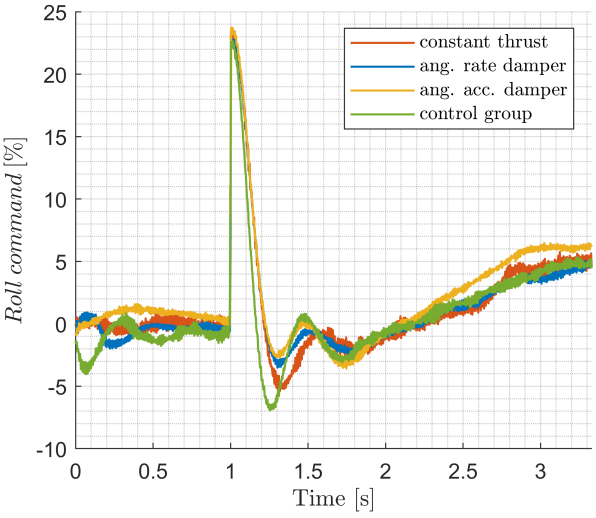

(b)

Fig. 8. Roll step input in the hover phase.

Table 5. Practical results for intended step inputs and different strategies.

	Settling time	**Max. input command**	**Energy req. for t=[1-3.5]**
control group	0.89 [sec]	23.62 [%]	8.00 [%· s]
constant thrust	0.84 [sec]	23.56 [%]	8.96 [%· s]
ang. rate damper	0.84 [sec]	22.76 [%]	8.18 [%· s]
ang. acc. damper	0.81 [sec]	23.73 [%]	10.31 [%· s]

Table 4. Practical results for the different strategies for disturbance rejection.

	Max. ϕ_{error}	Max. input command	Relative change	Energy required for t=[0-2.25]
control group	5.19 [deg]	26.64 [%]	100 [%]	31.44 [%· s]
constant thrust	6.29 [deg]	31.67 [%]	119 [%]	40.38 [%· s]
ang. rate damper	5.79 [deg]	29.62 [%]	111 [%]	38.78 [%· s]
ang. acc. damper	6.92 [deg]	33.84 [%]	127 [%]	42.62 [%· s]

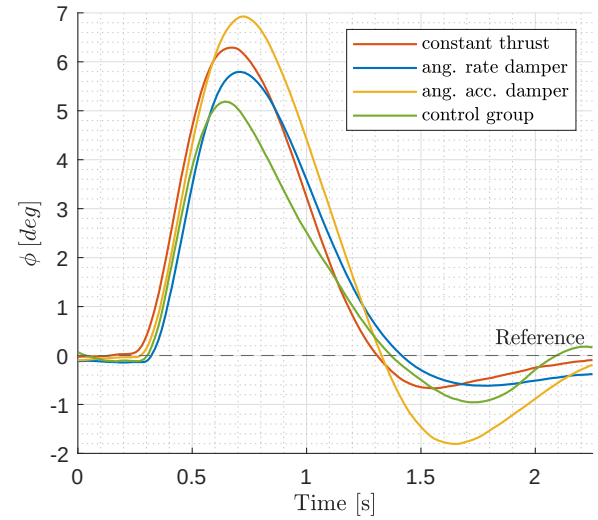

(a)

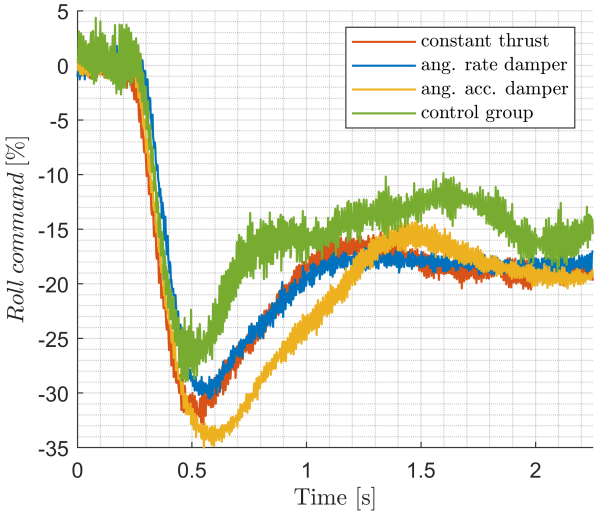

(b)

Fig. 9. Intended step disturbance rejection in the Hover phase.

6. Conclusion

This paper proposes a combined aerial system consisting of a biplane and quadrotor attached together, that can hover cooperatively, and disassemble in-flight followed by separate flight. In-flight release works consistently and is tested up to a forward pitch angle of -18 [deg]. Given the constraint of no intercommunication between the two vehicles, the angular rate damper control strategy for the quadrotor helps with disturbance rejection, while marginally affecting performance in terms of intended behavior. Compared to the control group strategy, no active attitude control would result in 19% extra command during the disturbance rejection experiment. With the rate damper strategy active, this is reduced to 11% extra input command needed. Also, the maximum angle that the joint platform reaches due to the disturbance and the total amount of energy required is reduced with the active damper strategy. The angular acceleration damper strategy performed significantly worse for both the extra input command and the maximum angle.

7. Discussion, further research

The system is designed to also be able to fly in fast forward flight, but this has not been tested within the scope of this paper. Future work could investigate the stability and tracking performance during transition and forward flight as well. Additionally, future work could examine how the quadrotor could be given more knowledge of the reference trajectory. If the quadcopter is programmed with the same flight plan and guidance laws, it could compute the same reference tracking errors as the biplane, given that it measures the same position. One could raise the question if it is worth it to avoid communication between the drones, as the results show that it does come at the cost of a small degradation in performance. Additionally, without communication the biplane may reach saturation limits quicker, as it has lower control authority compared to the case where it can send a command to the quadrotor. Communication would also allow for the quadrotor to adjust the thrust setting to the most efficient level, instead of the constant value that it had in this paper.

References

[1] Mark Voskuijl, Muhammad R Said, Jaspreet Pandher, Michel J van Tooren, and Blin Richards. In-flight deployment of morphing uavs–a method to analyze dynamic stability, controllability and loads. In *AIAA Aviation 2019 Forum*, page 3126, 2019.

[2] Daniel Briggs Wilson, Ali Göktogan, and Salah Sukkarieh. Guidance and navigation for uav airborne

docking. In *Robotics: Science and Systems*, volume 3, 2015.

[3] Ruibin Xue and Gaohua Cai. Formation flight control of multi-uav system with communication constraints. *Journal of aerospace technology and management*, 8(2):203–210, 2016.

[4] Mohammad A Dehghani and Mohammad B Menhaj. Communication free leader-follower formation control of unmanned aircraft systems. *Robotics and Autonomous Systems*, 80:69–75, 2016.

[5] David Saldana, Bruno Gabrich, Guanrui Li, Mark Yim, and Vijay Kumar. Modquad: The flying modular structure that self-assembles in midair. In *2018 IEEE International Conference on Robotics and Automation (ICRA)*, pages 691–698. IEEE, 2018.

[6] Raymond Oung and Raffaello D'Andrea. The distributed flight array: Design, implementation, and analysis of a modular vertical take-off and landing vehicle. *The International Journal of Robotics Research*, 33(3):375–400, 2014.

[7] David Saldana, Parakh M Gupta, and Vijay Kumar. Design and control of aerial modules for inflight self-disassembly. *IEEE Robotics and Automation Letters*, 4(4):3410–3417, 2019.

[8] Atheer L. Salih, M. Moghavvemi, Haider A. F. Mohamed, and Khalaf Sallom Gaeid. Modelling and pid controller design for a quadrotor unmanned air vehicle. In *2010 IEEE International Conference on Automation, Quality and Testing, Robotics (AQTR)*, volume 1, pages 1–5, 2010.

[9] Hongwei Mo and Ghulam Farid. Nonlinear and adaptive intelligent control techniques for quadrotor uav–a survey. *Asian Journal of Control*, 21(2):989–1008, 2019.

[10] Christophe De Wagter, Bart Remes, Ewoud Smeur, Freek van Tienen, Rick Ruijsink, Kevin van Hecke, and Erik van der Horst. The nederdrone: A hybrid lift, hybrid energy hydrogen uav. *international journal of hydrogen energy*, 46(29):16003–16018, 2021.

[11] Hang Zhang, Bifeng Song, Haifeng Wang, and Jianlin Xuan. A method for evaluating the wind disturbance rejection capability of a hybrid uav in the quadrotor mode. *International Journal of Micro Air Vehicles*, 11:1756829319869647, 2019.

[12] Bart Theys, Cyriel Notteboom, Menno Hochstenbach, and Joris De Schutter. Design and control of an unmanned aerial vehicle for autonomous parcel delivery with transition from vertical take-off to forward flight. *International Journal of Micro Air Vehicles*, 7(4):395–405, 2015.

[13] Ewoud JJ Smeur, Guido CHE de Croon, and Qiping Chu. Cascaded incremental nonlinear dynamic inversion for mav disturbance rejection. *Control Engineering Practice*, 73:79–90, 2018.

[14] Ewoud JJ Smeur, Qiping Chu, and Guido CHE de Croon. Adaptive incremental nonlinear dynamic inversion for attitude control of micro air vehicles. *Journal of Guidance, Control, and Dynamics*, 39(3):450–461, 2016.

[15] Robert Mahony, Vijay Kumar, and Peter Corke. Multirotor aerial vehicles: Modeling, estimation, and control of quadrotor. *IEEE Robotics and Automation magazine*, 19(3):20–32, 2012.

[16] EJJ Smeur. *Incremental Control of Hybrid Micro Air Vehicles*. PhD thesis, Delft University of Technology, 2018.

[17] Hikaru Otsuka, Daisuke Sasaki, and Keiji Nagatani. Reduction of the head-up pitching moment of small quad-rotor unmanned aerial vehicles in uniform flow. *International Journal of Micro Air Vehicles*, 10(1):85–105, 2018.